

SEISMIC RESPONSE AND FAILURE MECHANISM OF FLEXIBLY SUPPORTED LIQUID STORAGE TANKS

W WUNDERLICH¹, C SEILER², J SCHWARZ³ And J HABENBERGER⁴

SUMMARY

This paper deals with the dynamic behavior of flexibly supported liquid-filled storage tanks under earthquake excitation. A simplified mechanical model is proposed to simulate the characteristics of the surrounding soil with its energy absorbing properties. In addition, a quasistatic approach is presented to analyse certain types of instability phenomena. Some examples which are verified by more detailed investigations in the time domain give insight into the particular dynamic behavior of these tanks. The results are also compared to those obtained by the current design procedure provided in the current draft of EC8, part 4.

INTRODUCTION

The dynamic characteristics of liquid filled storage tanks under earthquake excitation are mainly determined by the interactive motion of the tank with the liquid and the soil. Therefore, a realistic assessment of the dynamic behavior of these tanks requires the inclusion of the liquid and the soil to ensure a safe but nevertheless economical design. However, some earthquake hazards have demonstrated that the approximations that are actually used in engineering practice are not based satisfactorily on the real behavior of these tanks. Thus, better procedures have to be developed to overcome these discrepancies.

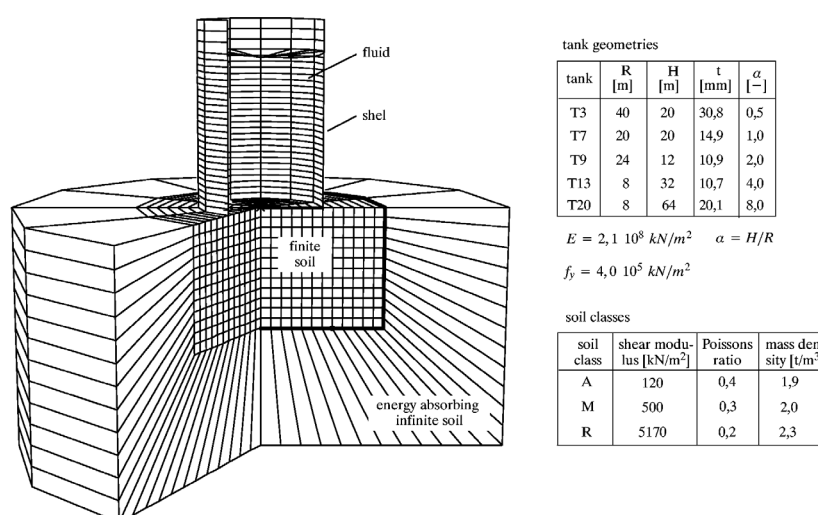


Figure 1: Soil-fluid-structure system

The methods of analysis may be roughly divided into two classes, the direct methods and the modal methods. Using the direct time integration a computational model (Figure 1) is described in [7] which has been successfully used for the complete dynamic analysis taking into account also the nonlinear effects in the shell

¹ Lehrstuhl für Statik, Technische Universität München, München, Germany Email: ww@statik.bauwesen.tu-muenchen.de

² Lehrstuhl für Statik, Technische Universität München, München, Germany seiler@statik.bauwesen.tu-muenchen.de

³ Inst. für konstruktiven Ingenieurbau, Bauhaus-Universität Weimar, Weimar, Germany : jochen.schwarz@bauing.uni-weimar.de

⁴ Institut für konstruktiven Ingenieurbau, Bauhaus-Universität Weimar, Weimar, Germany : habenber@bauing.uni-weimar.de

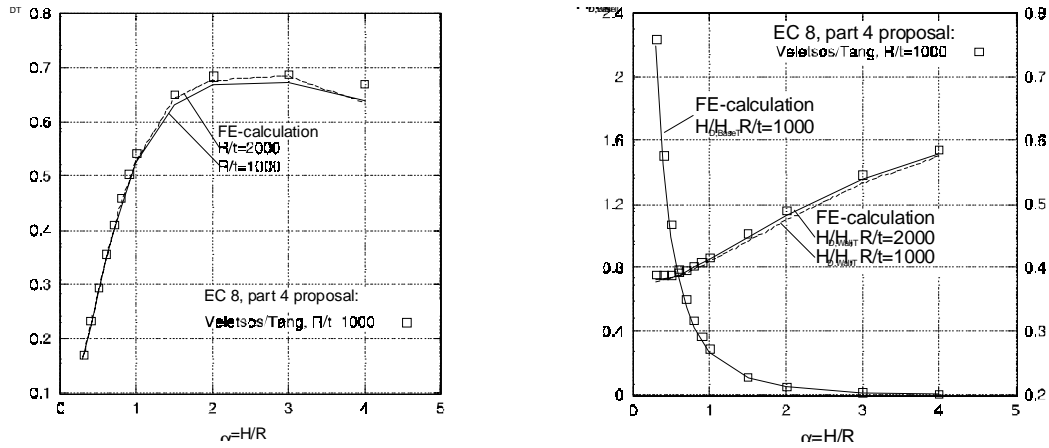


Figure 4: Normalized masses M_D and heights H_D : comparison of FE-calculations with EC 8, part 4 proposal [12]

In Figure 3 and 4 the normalized masses, heights and coefficients for the natural frequency of the impulsive flexible pressure component given by Veletsos and Tang [6] and proposed in the EC 8, part 4 [12] are compared with those obtained by numerical calculations using the FE-model [7] according to Figure 1. The 1st natural circular frequency can be determined by the coefficients C_1 with the formula [6]:

$$\omega_1 = \frac{C_1}{H} \sqrt{\frac{E}{\rho}} \quad (1)$$

(H height of the tank, E Young's modulus, ρ density of the shell)

Foundation-soil subsystem:

The proposed simplified methods in EC8, part 4 [12] assume that the tank rests on the half-space with a rigid circular base mat. However, the tank base is a thin steel sheet with very small bending stiffness. The foundation stiffness can be estimated with the parameter $\delta = K/(GR^3)$ (K bending stiffness of the base plate, G shear modulus of the soil, R radius of the tank). Values of δ are in the range of 10^{-10} to 10^{-5} for typical constructions of liquid storage tanks.

For the determination of the tank-soil interaction only the unconstrained half-space surface subjected to the hydrodynamic pressure and the ring load of the tank wall is considered since the bending stiffness of the foundation can be neglected. According to Hampe et.al. [2] the horizontal motion is not influenced by the foundation stiffness and modifications occur only for the rocking motion. Assuming that the rocking and the horizontal motion are uncoupled the relation between total base moment MM_T and the rotation of the tank base ψ is given by the rocking impedance function:

$$MM_T = K_R [k_R + ia_0 c_R] \psi \quad (2)$$

$$(K_R = \frac{8 GR^3}{3(1-\nu)}; a_0 = \frac{\Omega R}{v_S}; v_S \text{ shear wave velocity; } \nu \text{ Poisson's ratio of the soil})$$

For the derivation of the rocking impedance function the following additional assumptions were introduced in case of the free half-space surface:

The total moment MM_T acting on the tank base has to be divided into the wall moment MM_W and the base moment MM_B . The ratio of these moments is nearly independent of the pressure component but varies with the slenderness ratio $\alpha = H/R$ of the tank.

The radial distribution of the base pressure can be described with a modified Bessel-function of first kind and order: $p(\zeta) = I_1(\pi/(2\alpha)\zeta)$, $\zeta = r/R$.

The load activated by the tank wall is distributed over a ring with thickness of $0.02R$.

The response of the tank depends on the vertical displacement of the half-space surface below the tank wall. The hydrodynamic pressure is hardly influenced by the relative deformation of the tank base.

In Figure 5 the coefficients k_R and c_R for $\nu = 0.333$ are compared to those of a rigid circular foundation.

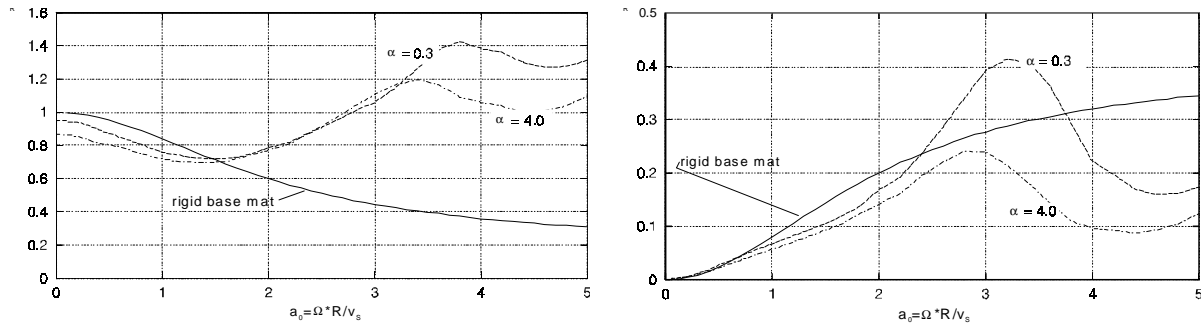


Figure 5: Spring and damping coefficients (k_R and c_R) of the rocking impedance function for $\nu=0.333$

Equivalent SDOF-system:

The rocking impedance function is implemented in the mechanical model as shown in Figure 2 using numerically determined masses, heights and frequencies of the shell-liquid subsystem. The radiation damping and the frequency modification of the coupled system were calculated according to the formulas given by Veletsos and Tang [6] for a tank series with constant volume of $19200m^3$ and for a ratio of radius to wall thickness of $R/t = 1000$. The tanks are supported by a soft soil with $v_s = 250m/s$ and $\nu = 0.333$. In Figure 6 the frequency shift and the radiation damping of an equivalent SDOF-system for the different foundation models are shown. The values obtained from numerical analysis using the FE-model [7] according to Figure 1 for a foundation stiffness of $\delta = 10^{-8}$ are compared with those for a rigid tank base and with the model of the free half-space surface.

For engineering application the coupled system according to Figure 2 can be replaced by a SDOF-oscillator (Figure 7) with adapted damping value \bar{D}_D and adapted natural frequency $\bar{\omega}_D$ [12]:

$$\bar{\omega}_D = \omega_D \eta \tag{2}$$

$$\bar{D}_D = D_S + D_R + \frac{D_D}{\eta^3} \geq D_D \tag{3}$$

(D_S material damping of the soil; D_D internal damping of the shell-liquid system)

The impulsive rigid component M_B can be considered approximately if the mass M_D is subjected to the absolute spectral acceleration. The sloshing pressure component is hardly affected by the interactive motion with the supporting soil and has to be applied without modifications. Whereas the differences in the frequency shifts are more pronounced for tall tanks ($\alpha \geq 1$) the main change of the radiation damping occurs for broad tanks ($\alpha < 1$). Concerning the radiation damping the current simplified design procedure in EC 8, part 4 delivers too optimistic values for flexibly supported broad tanks since the seismic response may be underestimated by the model with rigid base mat.

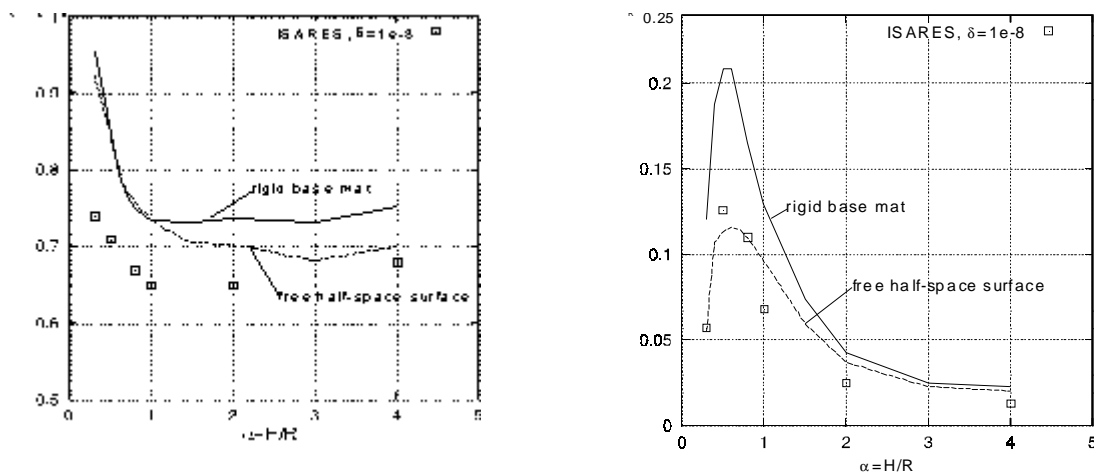


Figure 6: Frequency shift η and radiation damping D_R for different foundation models

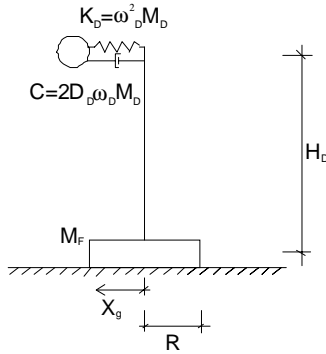


Figure 7: Equivalent oscillator with adapted properties for engineering application

QUASISTATIC APPROACH OF THE FAILURE MECHANISM

Instead of calculating the complete dynamic response by time integration a quasistatic approach presented in [9] may be employed to estimate the load carrying behavior of these tanks. The dynamic problem is then reduced to a static load case considering the linear modal pressure eigenforms as equivalent forces on the tank wall. As shown in [1] and according to the achieved results by the interactive model [7] this quasistatic approach is, in general, sufficient to predict the potential failure mechanisms of these tanks.

With respect to the different damage modes of the tank wall a number of different superpositions of the individual pressure contributions [9] have to be considered (Figure 8). They are the static pressure p_{stat} and the pressure due to vertical earthquake excitation, p_v , which are both axisymmetrically distributed, and the cosine distributed pressure due to the horizontal earthquake excitation, p_h . Employing a nonlinear finite element procedure the pressures are increased by a load multiplier λ which is then equivalent to the absolute horizontal acceleration a_h :

$$p = p_{stat} + \lambda [p_h \pm \frac{a_v}{a_h} p_v] \quad (4)$$

By variation of the ratio a_v/a_h the influence of the vertical earthquake component can be evaluated. Also higher pressure eigenforms than the first one may be considered in these calculations.

For cylindrical steel tanks the maximum seismic response could be limited by a number of possible failure modes including elastic buckling or material yielding due to the different action of the earthquake components (Figure 8). In this context, load case I is considered as most critical to elastic-plastic buckling. This failure mechanism results from the combined action of the high circumferential tensile stresses due to internal pressure and the axial compressive membrane stresses due to the overturning moment caused by the horizontal acceleration and leads to yielding in a narrow band in the tank wall. This elastic-plastic collapse, which is one of the most frequently observed failure modes, is called “elephant-footing“ according to its particular bulge form. For tank T9 (Figure 1) characterized by the slenderness parameter $\alpha = 2$ the buckling mode and the load carrying behavior are shown in Figure 9. The same buckling mode is observed for different ratios of a_v/a_h . However, the maximum load level λ which may be defined as critical for this instability phenomenon decreases with increasing hoop stresses due to the influence of the vertical earthquake component. After the turning point there is a drastic reduction of the load whereas the minimum load level is independent of the vertical component. This particular behavior results from a redistribution of the dominant meridional stresses which concentrate in those regions where the shell begins to bulge outward. A further discussion of the quasistatic behavior of these tanks may be found in [9].

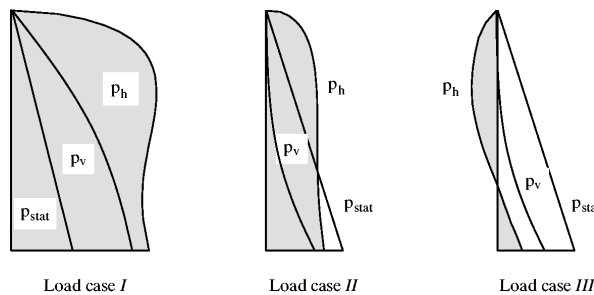


Figure 8: Different superpositions of the pressure contributions

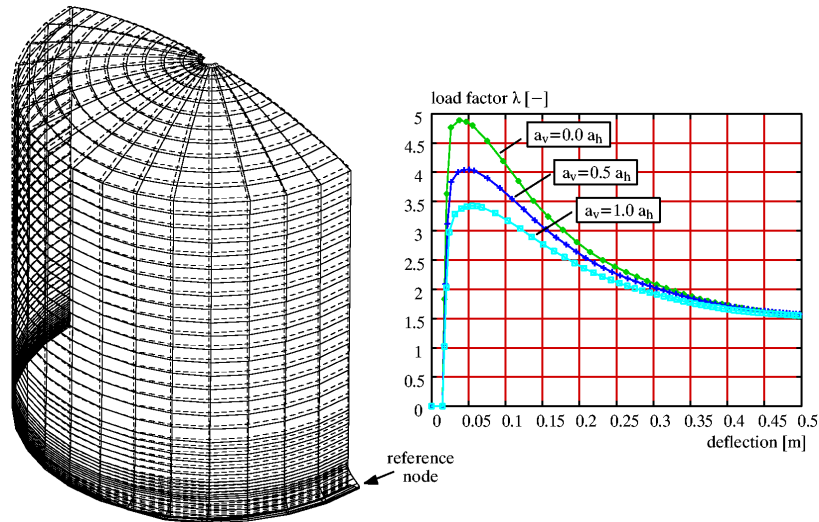


Figure 9: “Elephant-footing”, tank T9

On the basis of the interactive model [7] a small parameter study is performed for tank T9 to show the particular dynamic behavior using direct time integration. After loading the tank with the dead load and the hydrostatic fluid pressure the tank is subjected to the horizontal component of a strong motion earthquake denoted by I3M6H2. Additionally, the parameter λ is introduced to investigate different load intensities and to compare the results with those obtained by the quasistatic approach. Since the dynamic behavior may be considered sensitive to initial imperfections, additionally, the stability of the system is investigated by including geometric imperfections which are assumed in the shape of the buckling mode obtained by the quasistatic approach.

With the characteristic properties of the equivalent oscillator (Figure 7) the spectral absolute acceleration of the dominant first pressure eigenform is found to be $a_h=2,42 \text{ m/s}^2$. Due to the quasistatic analysis (Figure 9) predicting a maximum load step of $a_h=4,85 \text{ m/s}^2$ no failure may be expected during earthquake excitation. This behavior becomes obvious regarding the history of the radial displacement of a node near the tank base oscillating in the linear range around the static state position (Figure 10). By varying the amplitude of the free-field excitation, however, a qualitative change in the displacement history may be detected for $\lambda = 2,0$. After a few seconds of the earthquake motion the displacements jump to another mean value and indicate an irreversible bulge deformation near the bottom edge. The resulting deformation pattern of the shell closely conforms to the buckling mode analysed by the quasistatic approach (Figure 9). Including geometric initial imperfections for $\lambda = 2,0$ no structural unstable behavior is identified so that dynamic instability can be excluded with respect to the assumed imperfections.

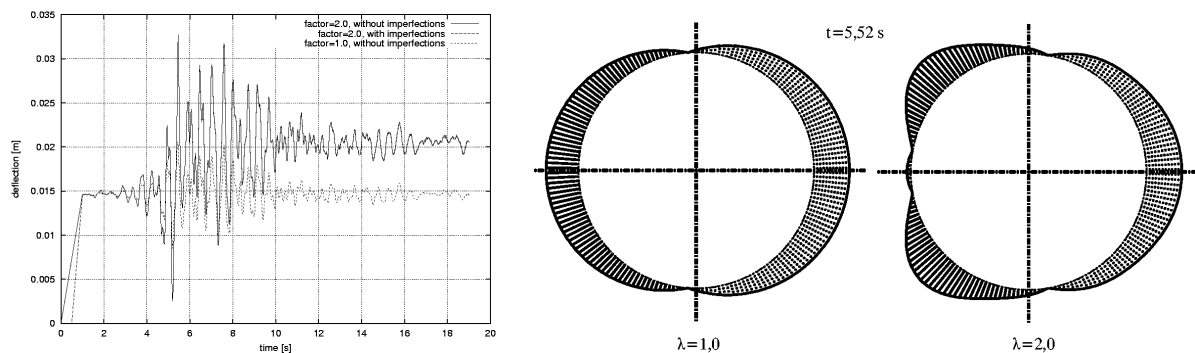


Figure 10: Radial displacement and distribution of the meridional stresses near the tank base

According to the quasistatic studies the load carrying behavior of tank T9 is dominated by the meridional stresses which result from the overturning moment due to the horizontal excitation. The redistribution of the axial stresses which occur at the maximum load step due to the quasistatic analysis is also observed in the time domain. This specific effect is shown in Figure 10 on an element near to the tank base for a load intensity of $\lambda = 1,0$ and $\lambda = 2,0$ at time step $t = 5.52 \text{ s}$ indicating the occurrence of irreversible deformations.

In the numerical model load case II is included in load case III and is considered as most critical with respect to elastic buckling due to the axial forces and the reduced stabilizing effect of internal pressure. However, this load case may also lead to elastic buckling in the upper tank wall due to external pressure as is shown in Figure 11 for tank T7 and $a_v = a_h$. This stability phenomenon results from compressive stresses in the circumferential direction caused by the load components acting as external pressure and exceeding the internal hydrostatic pressure. According to the cosine distributed pressure component due to the horizontal excitation the failure mode is concentrated in a restricted region of the tank wall. This phenomenon was also studied by the authors of [10] assuming, however, constant loading conditions in the circumferential direction.

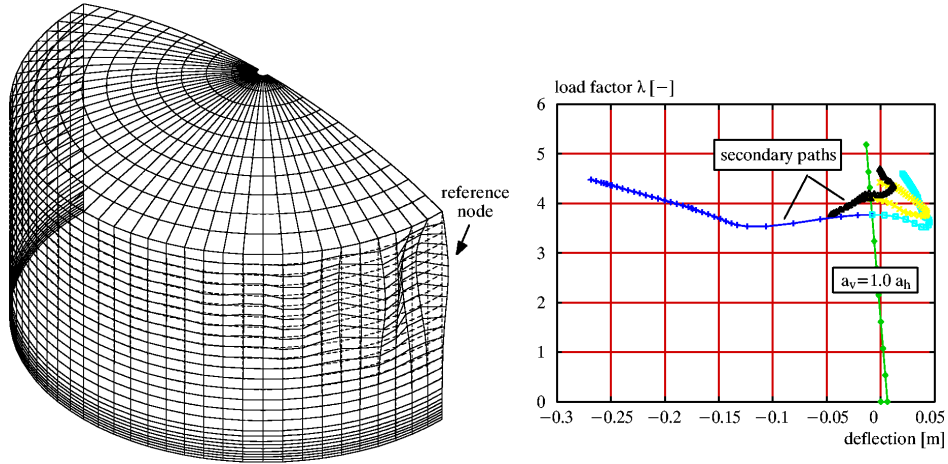


Figure 11: Elastic buckling in the upper tank wall, tank T7

For comparison with the design criteria of EC8, part 4 [12] it is important to note that all pressure components due to the horizontal and the vertical excitation cause compressive or tensile stresses in the circumferential direction whereas the first eigenform of the horizontal motion also leads to compressive and tensile stresses in meridional direction and to shear stresses. To consider these effects in a simplified design procedure the membrane stresses n_{22} and n_{12} which are cosine distributed in the circumferential direction may be approximated by simple equilibrium considerations applying the mass (M) and the moment (MM) due to chapter 0. The hoop stresses n_{11} are directly affected by the pressures activated by the horizontal (p_h), the vertical excitation (p_v) and static pressure p_{stat} :

$$n_{12} = \frac{M}{\pi R} a_h, \quad n_{22} = \frac{MM}{\pi R^2} a_h, \quad n_{11} = R[p_{stat} + p_h a_h + p_v a_v] \quad (5)$$

In the current draft of EC8, part 4 [12] two criteria have to be performed for stability verifications. In criterion I the allowable axial stresses are related to the classical buckling load under axial compression considering initial imperfections and the stabilizing effect of internal pressure. Criterion II was developed by Rotter, Seide [11] and gives an assessment of the meridional stresses required to initiate elastic-plastic collapse due to the biaxial stress state consisting of hoop tension and vertical compression. Assuming $a_v = 0,5a_h$ and applying the approximated stresses to the design rules critical horizontal accelerations may be achieved as shown in **Error! Reference source not found.** together with the results on the basis of the common design criterion for membrane yielding (criterion III). Comparing these accelerations with the numerical results (FE), only criterion II is qualitatively similar, but may be regarded as too conservative.

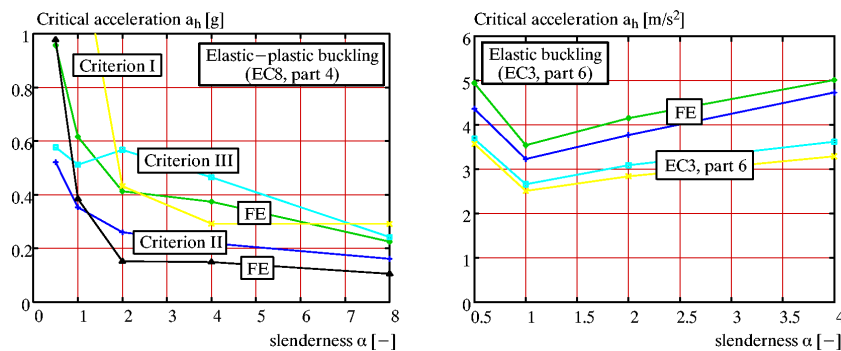


Figure 12: Comparison of current design rules and numerical results (FE)

The phenomenon of elastic buckling in the upper tank wall (**Figure** : 12) is not considered in the current draft of EC8, part 4. Applying, however, the approximated stresses to the design criterion of EC3, part 6 [13] for cylindrical shells under uniform external pressure and assuming $a_v=a_h$, critical accelerations qualitatively similar to the numerical results (FE) may be achieved.

CONCLUSIONS

1. For tank T9 subjected to horizontal earthquake excitation good agreement of the results obtained by the quasistatic approach and by more detailed evaluations in the time domain may be found.
2. The quasistatic results have to be verified with further research in the time domain considering the influence of the vertical earthquake component and the stability phenomenon of elastic buckling.
3. Due to the numerical results a modification of the current design practice would be advantageous in view of the analysed failure mechanisms and of economical considerations.
4. The consideration of a flexible tank base leads to a decrease of the resonance frequency of tall tanks ($\alpha \geq 1$) and to a decrease of the radiation damping of broad tanks ($\alpha < 1$).
5. The results obtained from the proposed simplified approach shows good agreement with those from numerical analysis.
6. Concerning frequency shift and radiation damping of liquid storage tanks with flexible base mat resting on soft soil the current design proposals underestimate the seismic response.

REFERENCES

1. Fischer, D., F. and Rammerstorfer, F. G. (1982), "The stability of liquid-filled cylindrical shells under dynamic loading", *Buckling of Shells*, E. Ramm (ed.), Springer-Verlag, pp. 569-597.
2. Hampe, E., Riedel, C. and Schwarz, J. (1990), "Ergebnisse von Experimenten und Berechnungen zur Boden-Bauwerk-Wechselwirkung", Institut für Industrie- und Spezialbau, Hochschule für Architektur und Bauwesen Weimar.
3. Haroun, M. A. and Housner, G. W. (1981) "Dynamic interaction of liquid storage tanks and foundation soil", *Proceedings of the 2nd ASCE/EMD Specialty Conference on Dynamic Response of Structures*, Atlanta, Georgia, pp. 346-360.
4. Lysmer, J. (1965), "Vertical motion of rigid footings", Ph. D. Dissertation, University of Michigan.
5. Schwarz, J., Habenberger, J., Wunderlich, W. and Seiler, Ch. (1998), "Critical loading conditions of anchored liquid storage tanks under earthquake excitation", *Proceedings of the 11th European Conference on Earthquake Engineering*, Paris.
6. Veletsos, A.S. and Tang, Y. (1990), "Soil-structure interaction effects for laterally excited liquid storage tanks", *Earthquake Engineering and Structural Dynamics*, Vol. 19, pp. 473-496.
7. Wunderlich, W., Schäpertöns, B. and Temme C. (1994), "Dynamic stability of nonlinear shells of revolution under consideration of the fluid-soil-structure interaction", *International Journal of Numerical Methods in Engineering*, Vol. 37, pp2679-2697.
8. Wunderlich, W., Springer, H. and Goebel, W. (1989), "Discretization and solution technique for liquid-filled shells of revolution under dynamic loading", *Discretization methods in structural mechanics*, Mang, H. A., Kuhn, G. (eds.), Springer-Verlag, Heidelberg, pp 145-155.
9. Wunderlich, W. and Seiler, C. (1998), "Nonlinear treatment of liquid-filled storage tanks under earthquake excitation by a quasistatic approach", *Advances in Computational Structural Mechanics*, B. H. V. Topping (ed.), Civil-Comp Press, pp283-291.
10. Staudinger, G. and Wohltan, S. (1987), "Manteldruckbeulen erdbebenbeanspruchter Tankbauwerke", Technical Report, Institut für Leichtbau und Flugzeugbau, Technische Universität Wien.
11. Rotter, J., M. and Seide, P. (1987), "On the design of unstiffened cylindrical shells subject to axial load and internal pressure", *Proceedings of the ECCS Colloquium on Stability of Plate and Shell Structures*, Ghent University, pp539-548.
12. ENV 1998-4, Eurocode 8, Part 4 (1998), "Design of structures for earthquake resistance – silos, tanks and pipelines".
13. prENV 1993-1-6, EC 3, Part 6 (1997), Design of steel structures – supplementary rules for the strength and stability of shell structures.